PERGAMON

International Journal of Heat and Mass Transfer 45 (2002) 4561–4575

International Journal of HEAT and MASS TRANSFER

www.elsevier.com/locate/ijhmt

Splashing of molten tin droplets on a rough steel surface

Saeid Shakeri, Sanjeev Chandra *

Department of Mechanical and Industrial Engineering, University of Toronto, 5 King's College Road, Toronto, Ont., Canada M5S 3G8

Received 15 February 2001; received in revised form 30 April 2002

Abstract

We photographed the impact of molten metal droplets on a flat plate. From these images we measured droplet dimensions during spreading and counted the number of fingers around a splashing drop. Experiments were done using stainless steel substrates with average roughness of 0.06, 0.07, 0.56, and 3.45 μm respectively. The temperature of the substrate was kept at either 25 or 240 °C. Droplet diameter (2.2 mm) and impact velocity (4 m/s) were kept constant, giving a Reynolds number (*Re*) of 31 135 and Weber number (*We*) of 463.

Raising substrate roughness from 0.06 to 0.56 μm enhanced the tendency of droplet to splash, whereas increasing roughness even further to 3.45 μm suppressed splashing. This behaviour was attributed to changes in droplet solidification rate with surface roughness. A simple model of droplet spreading was used to estimate thermal contact resistance between the droplet and surface. Increasing surface roughness was found to raise thermal contact resistance and reduce heat transfer from the droplet to the substrate, delaying the onset of solidification and reducing splashing. The number of fingers formed around a droplet splashing on a smooth surface could be predicted reasonably well by a model based on Rayleigh–Taylor instability theory. Increasing surface roughness reduced the number of fingers while enlarging their size.

1. Introduction

A liquid droplet splashes when it hits a solid body with sufficient velocity. Immediately after a droplet impinges on a surface a thin liquid film jets out radially from under it. Waves form along the edges of this film and if their growth is not damped out by fluid viscosity or surface tension they develop into long fingers that detach, producing small satellite droplets. Splashing is undesirable in industrial and agricultural processes such as spray-painting, spray-coating or application of pesticides on foliage. The aim in these applications is to cover a given surface area with the smallest possible volume of liquid. Increasing the impact velocity of spray droplets enlarges the area they cover after flattening out; there is a limit, however, as to how much we can raise droplet velocity before the onset of splashing. Once this happens most of the small satellite droplets that detach bounce off the surface, wasting material and creating pollution. It is therefore useful to be able to foresee, and consequently avoid, conditions that will make a droplet splash. But the threshold at which splashing occurs is difficult to predict since it is a complex function of droplet and surface properties.

Experiments in which impact of liquid drops was photographed [1–3] established that droplets splash when the "splash parameter"—a dimensionless function of the droplet diameter, impact velocity, density, viscosity and surface tension—exceeds a critical value. The value of the critical splash parameter depended not only on the properties of the droplet, but also those of the solid substrate. In particular, the substrate roughness is known to play an important role in splashing: increasing surface roughness promotes splashing of liquid droplets [4–6].

The physical mechanism that triggers splashing is still not entirely clear. Allen [7] first put forward the hypothesis that splashing is caused by Rayleigh–Taylor instability on the edges of the spreading liquid film.

* Corresponding author. Tel.: +1-416-978-5742; fax: +1-416-978-7753.

E-mail address: chandra@mie.utoronto.ca (S. Chandra).

0017-9310/02/$ - see front matter
PII: S0017-9310(02)00170-9

Nomenclature

c_p	specific heat
D	diameter of spreading droplet, measured at droplet-substrate interface
D_0	diameter of spherical droplet
D_{max}	maximum droplet diameter after spreading on the surface
k	thermal conductivity
KE_1	initial kinetic energy
ΔKE	kinetic energy loss due to solidification
N	number of fingers
R_a	average surface roughness
R_c	thermal contact resistance
s	thickness of solid layer
s^*	dimensionless thickness of solid layer ($= s/D_0$)
SE_1	droplet surface energy before impact
SE_2	droplet surface energy after impact
t	time
t^*	dimensionless time ($= tV_0/D_0$)
t_{max}	droplet spread time
T_m	melting temperature
V_0	droplet impact velocity
W	work done in deforming droplet

Greek symbols

σ	surface tension
μ	viscosity of drop
ρ	density of drop
θ	advancing liquid–solid contact angle
ξ	spread factor ($= D/D_0$)
ξ_{max}	maximum spread factor

Dimensionless numbers

Pr	Prandtl number ($= \mu c_p/k$)
Re	Reynolds number ($= \rho V_0 D_0/\mu$)
We	Weber number ($= \rho V_0^2 D_0/\sigma$)

Thoroddsen and Sakakibara [8] suggested that the instability might be triggered even before the droplet touches the solid plate, when it decelerates due to increased pressure in the air gap separating liquid and solid surfaces. Kim et al. [9] used Rayleigh–Taylor instability theory to predict the number of number of fingers formed around a drop and obtained reasonable agreement with experimental observations. Bussman et al. [10] used a three-dimensional computational fluid dynamics code to model droplet impact and splashing, and initiated the growth of fingers in their simulations by introducing a sinusoidal perturbation into the velocity field immediately after impact. They speculated that in reality protrusions on the surface disturb liquid flow, with the amplitude of the perturbation proportional to the magnitude of surface roughness.

When a molten droplet lands on a cold surface, its subsequent flow depends on the rate of heat transfer between the droplet and substrate. Rapid cooling of an impacting droplet can influence splashing via several mechanisms: viscosity and surface tension increase as the liquid cools [11] while solidification arrests the growth of fingers around a splat [12]. Both these effects tend to suppress splashing. On the other hand solidification along the edges of an impacting droplet can perturb liquid flow and promote splashing in much the same way as surface roughness [13].

Relatively few controlled laboratory studies have examined the splashing of droplets that are simultaneously freezing. Much of the literature on molten metal droplet impact is concerned with droplets that are deposited so gently that they remain intact while spreading on the surface [14–16]. Berg and Ulrich [17] dropped molten tin and lead drops onto flat plates of varying roughness. They measured the mass of the droplet lost due to splashing, and found increasing surface roughness led to greater loss of material. Bhola and Chandra [11] and Aziz and Chandra [12] photographed the splash of wax and tin droplets respectively on a stainless steel substrate and developed simple models to predict the maximum extent of droplet spread and the number of fingers formed during splashing; however all their tests were done with a single substrate whose roughness was kept constant.

The objective of this study was to photograph molten tin droplets splashing on stainless steel substrates and to determine the effect of substrate roughness and temperature on droplet impact dynamics. We varied substrate roughness from 0.06 to 3.45 μm. The substrate temperature was kept at either room temperature (~25 °C) or at 240 °C, which is above the melting point of tin. The initial droplet diameter (2.2 mm), temperature (246 °C) and velocity (4 m/s) were kept constant in all the tests giving a Reynolds number (Re) of 31 135 and Weber number (We) of 463. We measured the evolution of splat diameter during droplet impact and counted the number of fingers formed around the edges of the splat.

2. Experimental method

Fig. 1 shows a schematic diagram of the experimental apparatus used to produce molten metal droplets and photograph their impact. The droplet generator consisted of a 50.8 mm diameter by 50.8 mm long stainless steel cylinder, through which was bored a 22.2 mm

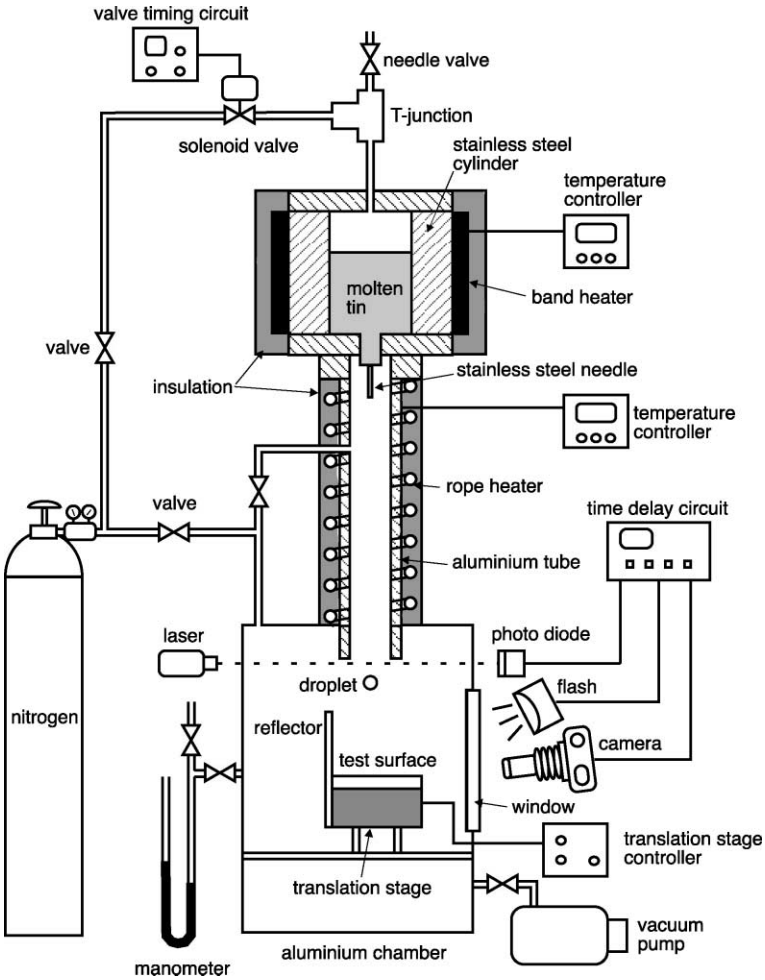

Fig. 1. Schematic diagram of the experimental apparatus.

diameter hole. Both upper and lower ends of the cylinder were capped with 6.4 mm thick discs. Around the cylinder was clamped a 400 W band heater. The temperature of the droplet generator was held constant at 250 °C, above the melting point of tin (232 °C), by regulating the heater with a temperature controller. The temperature of the droplet generator was measured with a K-type (chromel–alumel) thermocouple inserted into a hole drilled into the steel cylinder. The cavity in the droplet generator was filled with tin pellets (99.8% pure Aldrich Chemical Co., Milwaukee, WI.).

A 12 mm long stainless steel needle with an outer diameter of 1.588 mm and inner diameter of 0.254 mm was inserted thorough the bottom plate of the droplet generator using a Swagelok bulkhead fitting. The bore of the tube was too small for the molten metal to flow though it under the effect of gravity alone and droplets were forced out by applying pressure pulses from a nitrogen tank. The pressure of the nitrogen supply line was maintained at 69 kPa and the pressure pulse was delivered by activating a solenoid valve for a duration of 10 ms. It was difficult to open and close the solenoid valve sufficiently rapidly to eject individual droplets on demand. To relieve the pressure inside the chamber promptly the gas line was connected to the droplet generator chamber through a stainless steel T-junction, one of whose outlets was connected to the upper plate of the droplet generator while the other was open to the atmosphere through a needle valve. When a gas pulse was applied sufficient pressure built up inside the chamber to force out a single droplet. The gas then escaped to the atmosphere though the vent, relieving the pressure inside the chamber and preventing further droplets from escaping. By adjusting the opening of the needle valve through which the gas was vented the size of droplets produced could be varied. All tests described in this paper were done with 2.2 mm diameter tin droplets.

Droplets fell after detachment through a 25.4 mm diameter aluminium tube that was heated using a 125 W rope heater around which ceramic fibre insulation was wrapped. In experiments the temperature of the tube varied from 250 °C at its top to 50 °C at the bottom, which was sufficient to prevented the droplets from freezing before they landed on the test surface. Calculation of heat loss from droplets during their fall [18] showed that their temperature at the moment of impact was 246 °C. The tip of the droplet generator needle was 0.815 m above the test surface, giving an impact velocity of 4.0 m/s.

Molten tin oxidizes rapidly in air; to prevent oxidation experiments were conducted in a nitrogen atmosphere. The test surface was placed inside an aluminium chamber (0.3 m × 0.3 m × 0.15 m in size) that was first evacuated with a vacuum pump and then filled with nitrogen. To preventing air from seeping into the chamber a slight positive pressure was maintained inside it during experiments. This was done by maintaining a small flow of nitrogen into the chamber that was allowed to leak out through an adjustable valve in the side of the chamber. A water manometer was used to measure the pressure inside the chamber and ensure that it remained constant. The gauge pressure was kept at 10 mm H_2O in all experiments.

The test surfaces on which droplets landed were 50.8 mm square and 6.4 mm thick stainless steel plates that were bolted to a copper block in which were inserted two 125 W cartridge heaters. A chromel–alumel thermocouple was inserted into a hole drilled into the test surfaces and used to measure their temperature. A temperature controller regulated the heaters in the copper block so as to maintain the test surface temperature constant within ±1 °C before a droplet was deposited on it.

Surface roughness measurements were done using a PDI Surfometer Series 400 (Precision Devices, Inc., Milan, MI), which records the surface profile of a component by running a stylus over it. It gives a value of the average roughness (R_a) over the sampling length, defined as the mean deviation of surface irregularities measured from a hypothetical perfect plane. We varied R_a from 0.06 to 3.45 μm by employing different methods of finishing the stainless steel plates. The lowest average surface roughness (0.06 μm) was achieved by polishing the surface with 0.3 μm alumina powder on a metallurgical rotating wheel. A surface with average roughness of 0.07 μm was obtained by polishing the surface with 600-grit emery cloth. Grit blasting was used to produce surfaces with higher roughness. A surface with average roughness of 0.56 μm was prepared by grit blasting it with a 60–100 grit aluminium oxide/glass bead mix. For surfaces with average roughness of 3.45 μm we used 0.6–2.0 mm diameter alumina particles.

Droplet impact was photographed using a single shot flash photographic method [12]. As a droplet fell to the substrate it passed through the beam of a 0.95 mW helium-neon laser, which was directed onto a photo diode. Interruption of the laser beam decreased the output voltage of the photo diode, which was detected by a timing circuit. The timing circuit first opened the shutter of a Nikon E3 digital camera with a 105 mm lens and then started a time delay circuit with 1 μs resolution. After a pre-set time had elapsed the time delay circuit sent a signal to trigger an electronic stroboscope flash with a 8 μs flash duration taking a single digital photograph of a droplet colliding with a surface. By varying the time delay between release of the droplet and triggering of the flash, different stages of droplet impact were photographed and the entire impact pieced together from this sequence of photographs. There was some slight variation in splat shape from one drop to the next, even when impact conditions were kept constant, since splashing is a random process affected by small variations in local surface conditions. Photographs presented in this paper are representative of typical splat shapes.

Measurements of droplet dimensions were made from digital images on a computer with image analysis software, using a picture of a 3.16 mm steel ball bearing as a calibration scale. Droplet measurements were accurate within ±0.06 mm.

3. Results and discussion

3.1. Droplet impact dynamics on a cold surface

Fig. 2 is a sequence of photographs showing the deformation of a 2.2 mm diameter tin droplet impacting on a flat plate with a velocity of 4 m/s. It landed on a stainless steel surface with 0.06 μm roughness at a temperature of 25 °C. The temperature of the droplet before impact was calculated [18] to be 246 °C, which is well above the melting point of tin (232 °C). The time (t) given below each image in Fig. 2 is measured from the instant that the droplet first made contact with the substrate. The reflected image of the droplet can be seen in the polished surface. In subsequent frames we can see the droplet spread radially until it reached its maximum spread at approximately 2.0 ms. After this time outward motion of the spreading rim was arrested and surface tension pulled the liquid part slightly inward until finally the droplet solidified completely at approximately 7 ms. A number of small fingers were observed around the rim of the droplet immediately after impact. A few broke off very soon after being formed (see $t = 0.2$ and 0.3 ms), but the rest became larger. However, solidification arrested further growth of these fingers and they did not detach.

Fig. 3 shows the effect of increasing surface roughness on droplet impact. Each column in the figure

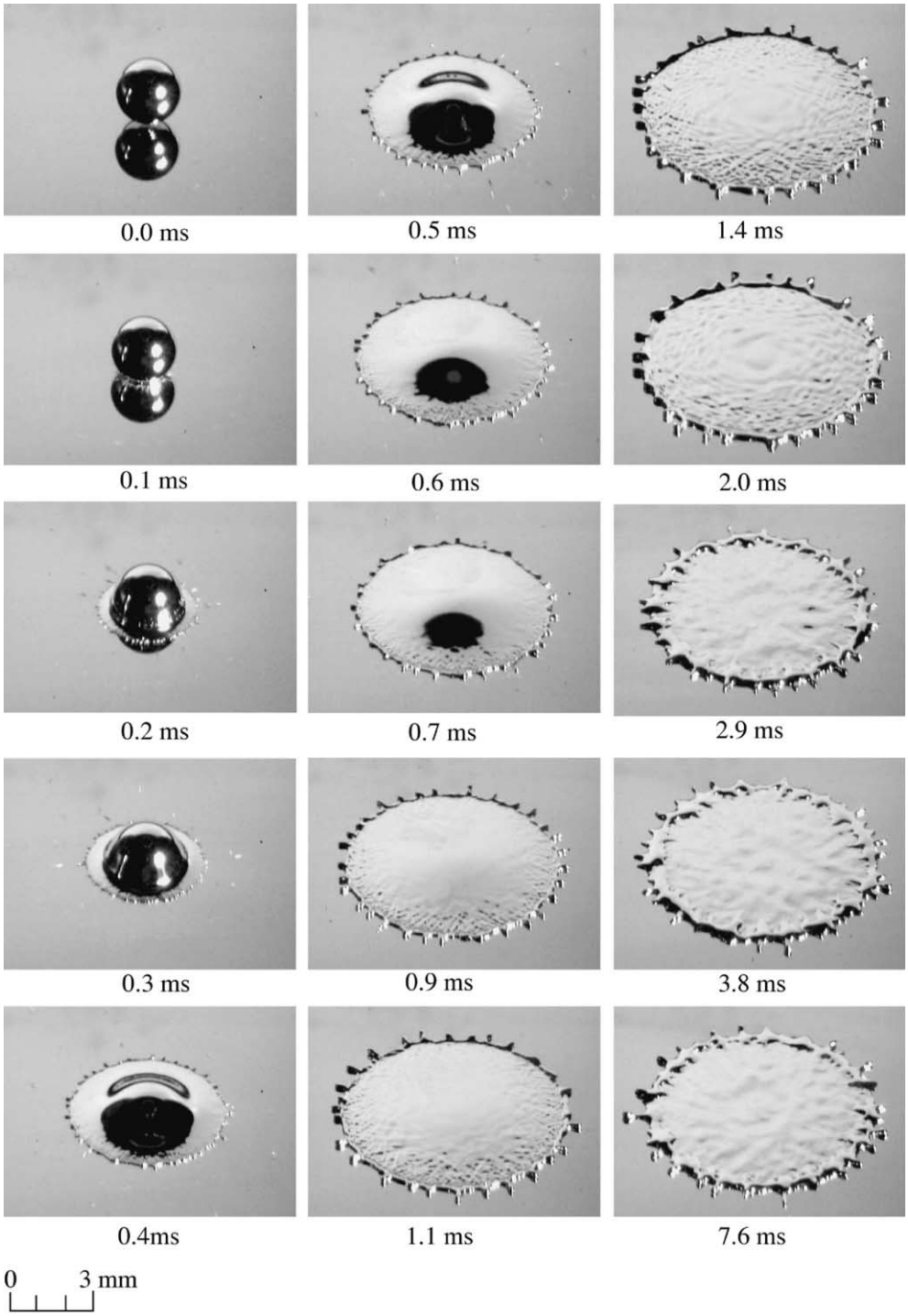

Fig. 2. The impact of 2.2 mm diameter molten tin droplet with 4.0 m/s velocity on a stainless steel plate at a temperature of 25 °C with surface roughness $R_a = 0.06$ μm.

shows the impact of a tin droplet on a surface of different roughness, with R_a of 0.07, 0.56, and 3.45 μm respectively. The time after impact is indicated on the left side of the images. During impact on a surface with

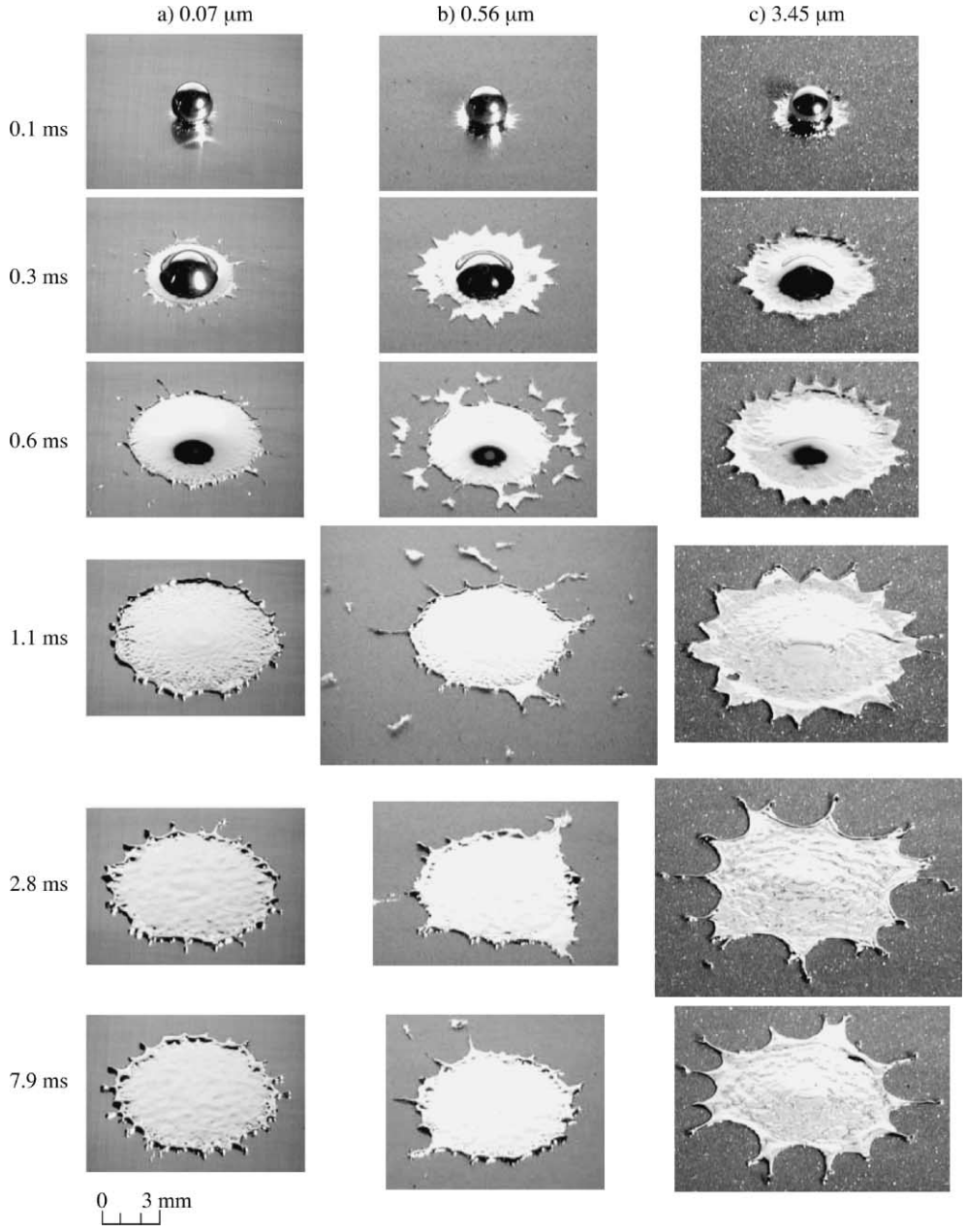

Fig. 3. The impact of 2.2 mm diameter molten tin droplets with 4.0 m/s velocity on a stainless steel plate at a temperature of 25 °C with surface roughness R_a: (a) 0.07 μm, (b) 0.56 μm, and (c) 3.45 μm.

roughness 0.07 μm small fingers were observed around the periphery of the drop immediately after impact (see $t = 0.1$ ms). Some of these detached forming satellite droplets ($t = 0.6$ ms). We did not observe as many satellite droplets on the surface with $R_a = 0.06$ μm (see Fig. 2) suggesting that their formation is very dependent on surface roughness. Experiments with liquid droplets [4,6] has shown that splashing is most sensitive to surface roughness when the value of roughness is very low. The splat reached its maximum spread at about 2 ms, about the same time as that seen for a surface with 0.06 μm surface roughness (see Fig. 2).

Increasing the roughness of the stainless steel substrate to $R_a = 0.56$ μm produced significant changes in droplet spreading, as seen in the second column of Fig. 3. Instead of thin fingers there were large, triangular

projections around the periphery of the drop early during spreading ($t = 0.3$ ms). Since they were very irregular it was not possible to meaningfully count the number of fingers, as we could in the case of a smooth surface (Fig. 2). The fingers then broke loose ($t = 0.6$ ms) and continued to travel outwards, leaving behind a solidified circular splat ($t = 7.9$ ms).

Increasing the roughness even further to $R_a = 3.45$ μm produced further changes in the droplet shape during spreading (Fig. 3c). Again there were triangular projections around the drop ($t = 0.3$ ms), but these did not detach ($t = 1.1$ ms). In this case solidification of the droplet was much slower, so that it remained liquid and surface tension forces pulled back the edge of the droplet ($t = 7.9$ ms). As it recoiled some droplets formed at the tips of the triangular finger and detached. The final splat had a distinctive star-like shape.

A quantitative description of droplet spreading can be given by measuring the evolution of splat diameter with time. For purposes of comparison the splat diameter (D) was measured from the roots of the fingers around its periphery. For irregular shaped splats we measured the splat diameter along 4 axes (horizontally, and at 45° and 90° to the horizontal) and averaged the measurements. Splat-to-splat variations in measurements of D for the same impact conditions were less than ±10%. Dividing the splat diameter by the initial droplet diameter (D_0) gives a dimensionless "spread factor" ($\xi = D/D_0$). Fig. 4 shows the variation of spread factor for droplets impacting on four surfaces with varying roughness, plotted as function of the dimensionless time (t^*) defined by:

$$t^* = \frac{tV_0}{D_0} \tag{1}$$

where V_0 is the impact velocity. Increasing roughness from 0.06 to 0.56 μm had little effect on the spreading rate, but on a surface with $R_a = 3.45$ μm droplets reached a significantly greater maximum spread diameter before they recoiled.

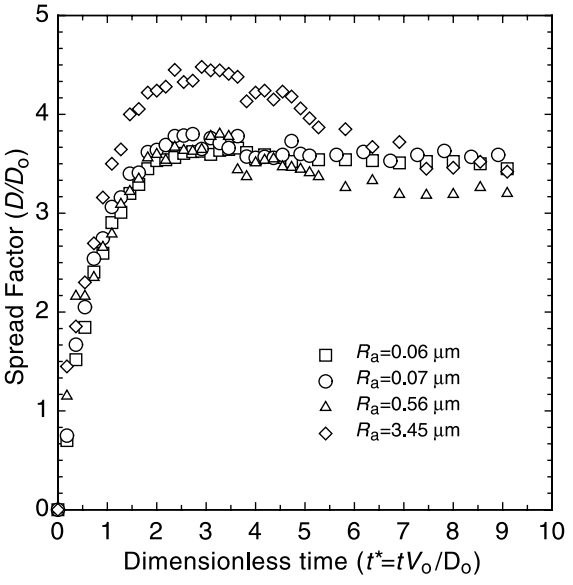

Fig. 4. Spread factor evolution for 2.2 mm diameter tin droplets impacting with 4 m/s velocity on a stainless steel surface with roughness R_a and 25 °C temperature.

3.2. Droplet impact dynamics on a hot surface

When a droplet lands on a cold surface, its spreading may be influenced by both surface roughness and surface temperature. To separate the effect of these two parameters, we repeated the impact experiments with the substrate heated to 240 °C, the same as the initial temperature of the molten droplet and above the melting point of tin ($T_m = 232$ °C). Impact was then essentially isothermal, with no solidification.

Fig. 5 shows the impact of a 2.2 mm diameter tin droplet with a velocity of 4 m/s on a stainless steel surface with $R_a = 0.06$ μm at a temperature of 240 °C. Fluid instability was seen as early as $t = 0.2$ ms around the edges of the drop, producing regularly spaced fingers around the edge of the drop. These fingers grew larger until the droplet reaches its maximum spread diameter at approximately $t = 2.3$ ms. At this stage, surface tension forces pulled the liquid towards the centre. As the liquid was pulled back the tips of the fingers detached ($t = 12.7$ ms) and remained stationary on the surface. The final shape of the droplet can be seen at $t = 16.7$ ms, with a pool of liquid surrounded by a ring of satellite droplets.

Fig. 6 shows that the effect of increasing surface roughness on the impact of a droplet on a hot surface. Each column of photographs shows a sequence of photographs of droplets landing on surfaces of different surface roughness: 0.07, 0.56, and 3.45 μm, respectively. Impact on a surface with $R_a = 0.07$ μm was similar to that seen previously on the surface with $R_a = 0.06$ μm, though the fingers were less regularly spaced. As surface roughness was increased further to $R_a = 0.56$ μm the fingers became larger and fewer in number. Few satellite droplets detached during the recoil ($t = 16.7$ ms). Finally, on a surface with the highest value of $R_a = 3.45$ μm there was less recoil and very few satellite droplets.

Measurements of the splat diameter during spreading were made from photographs and the results are shown in Fig. 7, plotted on dimensionless axes. On a surface at 240 °C there was little effect of surface roughness on droplet spreading, unlike what was found earlier for a surface at 25 °C (see Fig. 4). Fig. 8a–d compares droplet spread diameters on each of the four surfaces used in

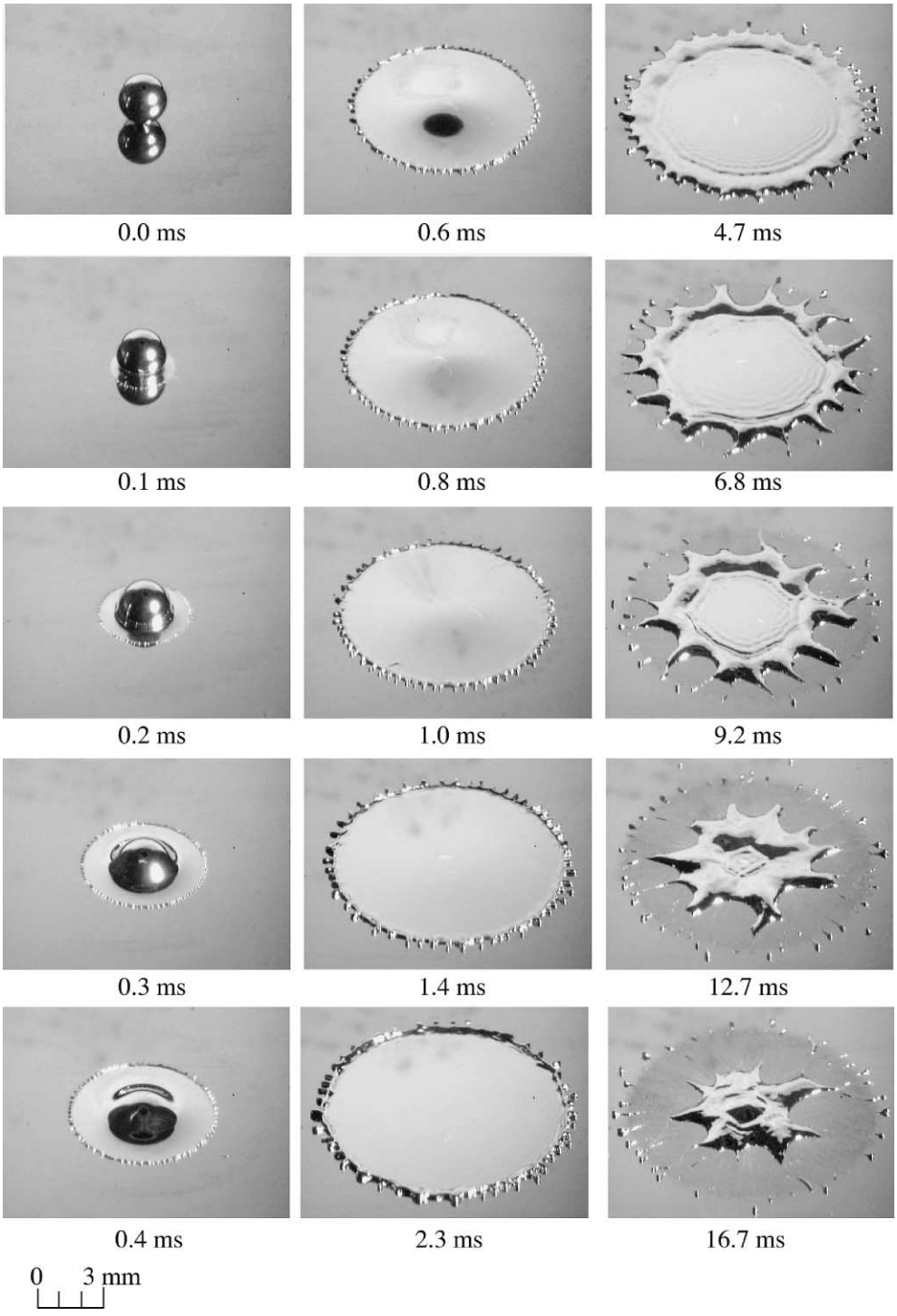

Fig. 5. The impact of 2.2 mm diameter molten tin droplet with 4.0 m/s velocity on a stainless steel plate at a temperature 240 °C with surface roughness $R_a = 0.06$ μm.

experiments, at two temperatures: 25 and 240 °C. In all cases there was less spreading on the colder surface, showing that solidification arrests droplet motion before spreading is complete. However, the difference between

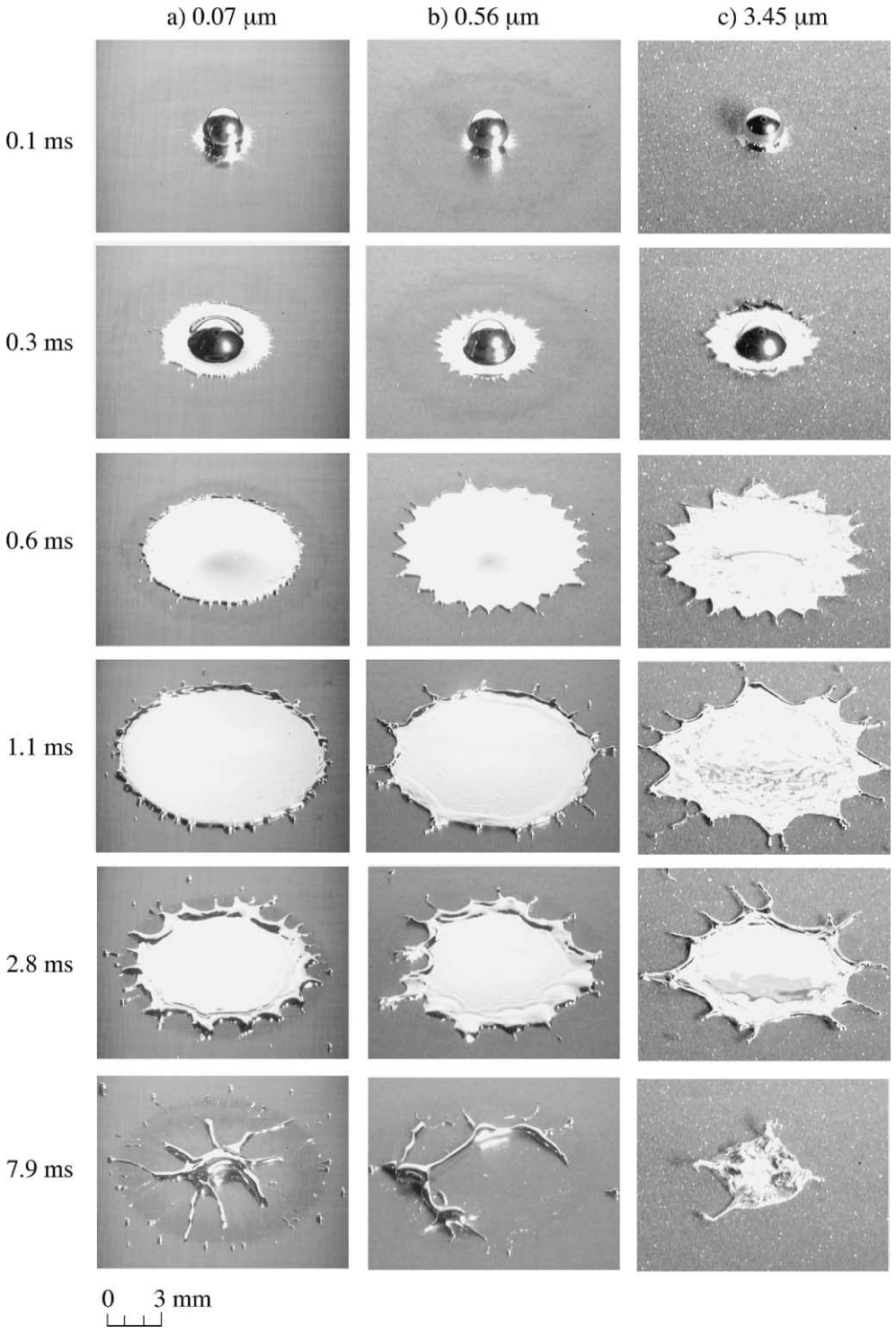

Fig. 6. The impact of 2.2 mm diameter molten tin droplets with 4.0 m/s velocity on a stainless steel plate at a temperature of 240 °C with surface roughness R_a: (a) 0.07 μm, (b) 0.56 μm, and (c) 3.45 μm.

maximum spread factors on surfaces at 25 and 240 °C was the least on the roughest surface with $R_a = 3.45$ μm (Fig. 8d). The effect of surface temperature on droplet spreading decreases as surface roughness increases.

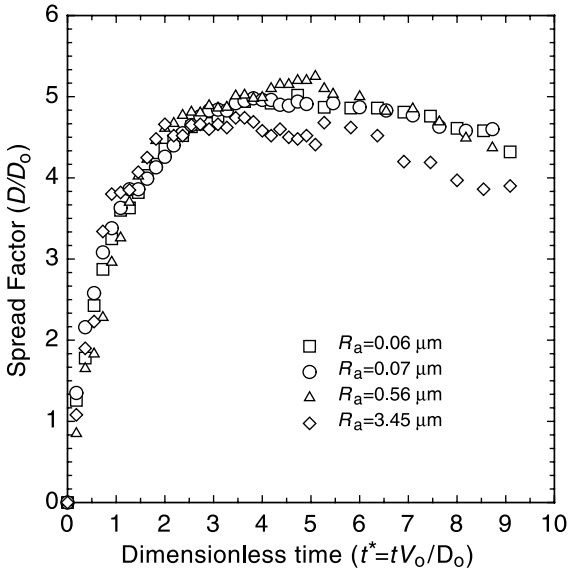

Fig. 7. Spread factor evolution for 2.2 mm diameter tin droplets impacting with 4 m/s velocity on a stainless steel surface with roughness R_a and 240 °C temperature.

3.3. Effect of surface roughness on droplet spreading

Increasing surface roughness can influence droplet spreading in three different ways:

(a) it can increase frictional losses during droplet spreading;
(b) it can trigger instabilities that cause fingering around the edge of the droplet;
(c) it can increase thermal contact resistance at the droplet-substrate interface due to trapped air in surface cavities.

The first of these effects did not seem important in our experiments. Fig. 7 shows that in the absence of solidification surface roughness has little effect on droplet spreading. However the role of surface roughness in creating instabilities in the flow seemed to be significant. Figs. 3 and 6 both show an increase in the size of fingers with surface roughness.

The third effect of surface roughness—that of increasing contact resistance—also appeared to have an important effect on droplet spread. Fig. 9 shows the bottom and top views of tin splats from our experiments photographed after solidification. The splats were formed by 2.2 mm diameter tin droplets impacting with a velocity of 4 m/s which landed and solidified on stainless steel surfaces at 25 °C with roughness of 0.06, 0.07, 0.56, and 3.45 μm, respectively. The splat formed on the smoothest plate ($R_a = 0.06$ μm) showed a small circular pattern at its centre, which appears to have solidified immediately after impact, and lines radiating out from the centre, showing the trajectory of liquid flow. Each line terminated in one of the fingers projecting from the droplet periphery, suggesting that fingers were initiated immediately after impact. Repeated experiments showed that every splat had the same pattern of lines under it. This supports the hypothesis [7,9] that fingers are formed immediately after the droplet contacts the substrate due to Rayleigh–Taylor instability. The splat formed on the $R_a = 0.07$ μm surface shows a similar pattern, though the central portion was larger, indicating that solidification was slightly later than in the previous case. The splat on the $R_a = 0.56$ μm surface showed an almost uniform bottom, indicating that the droplet had almost completely spread before it started to freeze. The splat landing on the roughest plate with $R_a = 3.45$ μm had an underside that conformed to the substrate, showing that it had time to fill in surface depressions before it froze.

On a smooth surface thermal contact resistance between the droplet and surface is low because little air is trapped in surface cavities. Therefore solidification is rapid, starting before the droplet has fully spread. Increasing surface roughness raises contact resistance, and lets the droplet spread to a greater extent before it freezes. This hypothesis explains why a droplet spread further on a rough surface than on a smooth surface (see Fig. 4) when the substrate temperature was low enough to cause freezing. On a hot surface, where there was no solidification, surface roughness had little effect on droplet spread (Fig. 7).

Thermal contact resistance also affects formation of satellite droplets. In Fig. 3 a large number of satellite droplets detached on the surface with $R_a = 0.56$ μm (see Fig. 3b, $t = 0.6$ ms), but not those with smaller or greater roughness (Fig. 3a and c). Surface roughness perturbs liquid flow and promotes formation of fingers. Numerical models of molten droplet impact [13] have shown that solidification assists this process, since frozen portions of the droplet rim also obstruct liquid flow. However, when surface roughness becomes very large it increases contact resistance and prevents freezing, decreasing detachment of satellite drops.

3.4. Estimate of thermal contact resistance variation with surface roughness

Pasandideh-Fard et al. [16] and Aziz and Chandra [12] estimated the value of thermal contact resistance between a stainless steel surface and an impacting tin droplet by measuring the surface temperature variation during droplet impact. They modelled droplet impact as two semi-infinite bodies suddenly brought together with a thermal resistance in between, and fit an analytical solution of the measured substrate temperature variation to calculate the contact resistance. Even though in reality the contact resistance will vary with time and

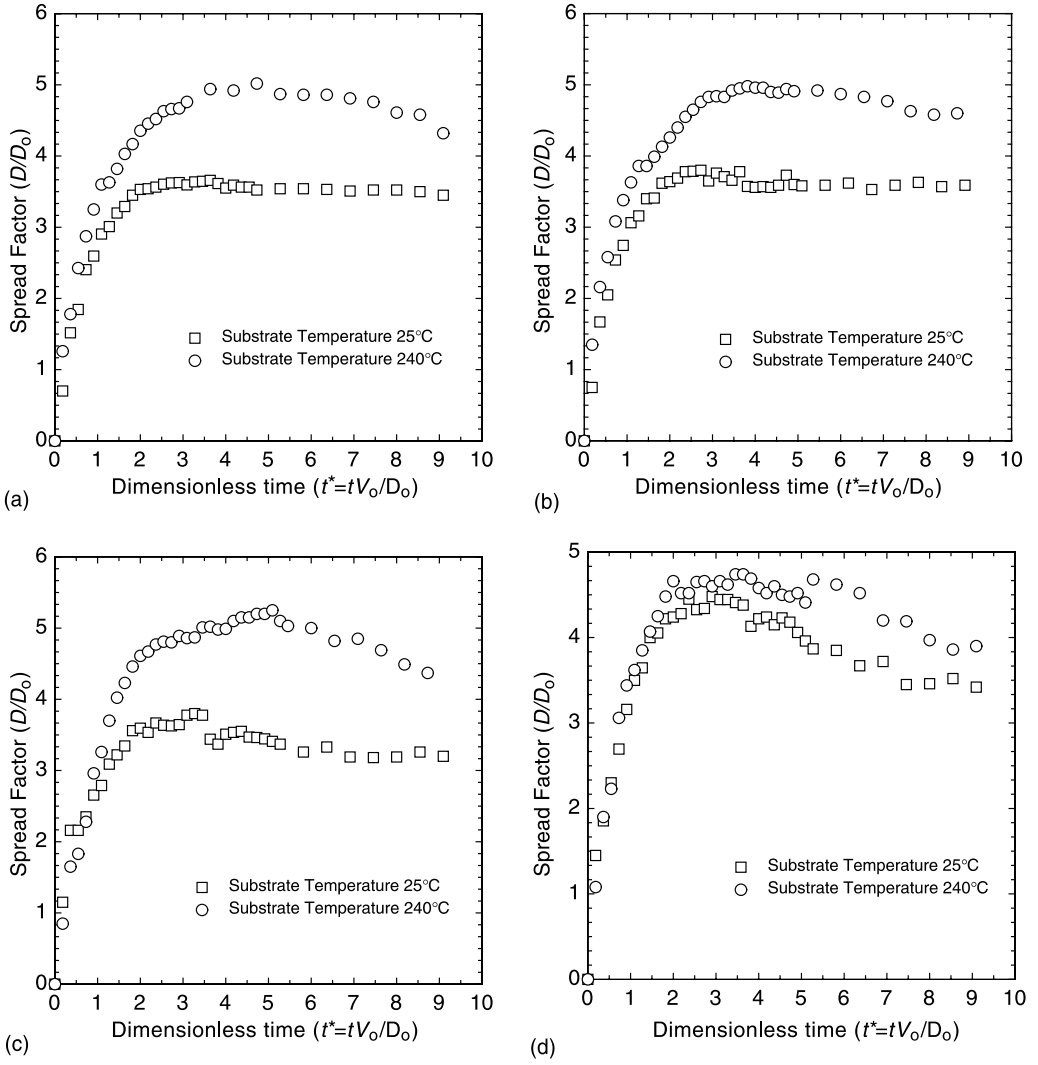

Fig. 8. Spread factor evolution for 2.2 mm diameter tin droplets impacting with 4 m/s velocity on stainless steel surfaces with a temperature of either 25 or 240 °C and surface roughness (R_a) of: (a) 0.06 μm, (b) 0.07 μm, (c) 0.56 mm, and (d) 3.45 μm.

position as the droplet spreads and solidifies, it was assumed to be constant (representing an average value). The contact resistance value was used in a simple energy conservation model to calculate the maximum splat diameter after impact.

We were unable to directly measure surface temperature variation on a roughened substrate, because grit blasting the surface destroyed the thermocouple junction. Instead, we estimated the thermal contact resistance indirectly by substituting our measured values of droplet spread diameter in the model of Pasandideh-Fard et al. [16]. To explain this procedure a brief description of their model is given below.

The model assumes that before impact the kinetic energy (KE_1) and surface energy (SE_1) of the droplet are given by:

$$KE_1 = \left(\frac{1}{2}\rho V_0^2\right)\left(\frac{\pi}{6}D_0^3\right) \tag{2}$$

$$SE_1 = \pi D_0^2 \sigma \tag{3}$$

After impact, when the droplet has reached its maximum spread diameter (D_{max}), its kinetic energy is zero, while its surface energy is:

$$SE_2 = \frac{\pi}{4}D_{max}^2\sigma(1-\cos\theta) \tag{4}$$

where θ is the advancing contact angle during spreading. The surface tension of tin was assumed to be constant, and changes with temperature were neglected. The contact angle was measured from photographs and

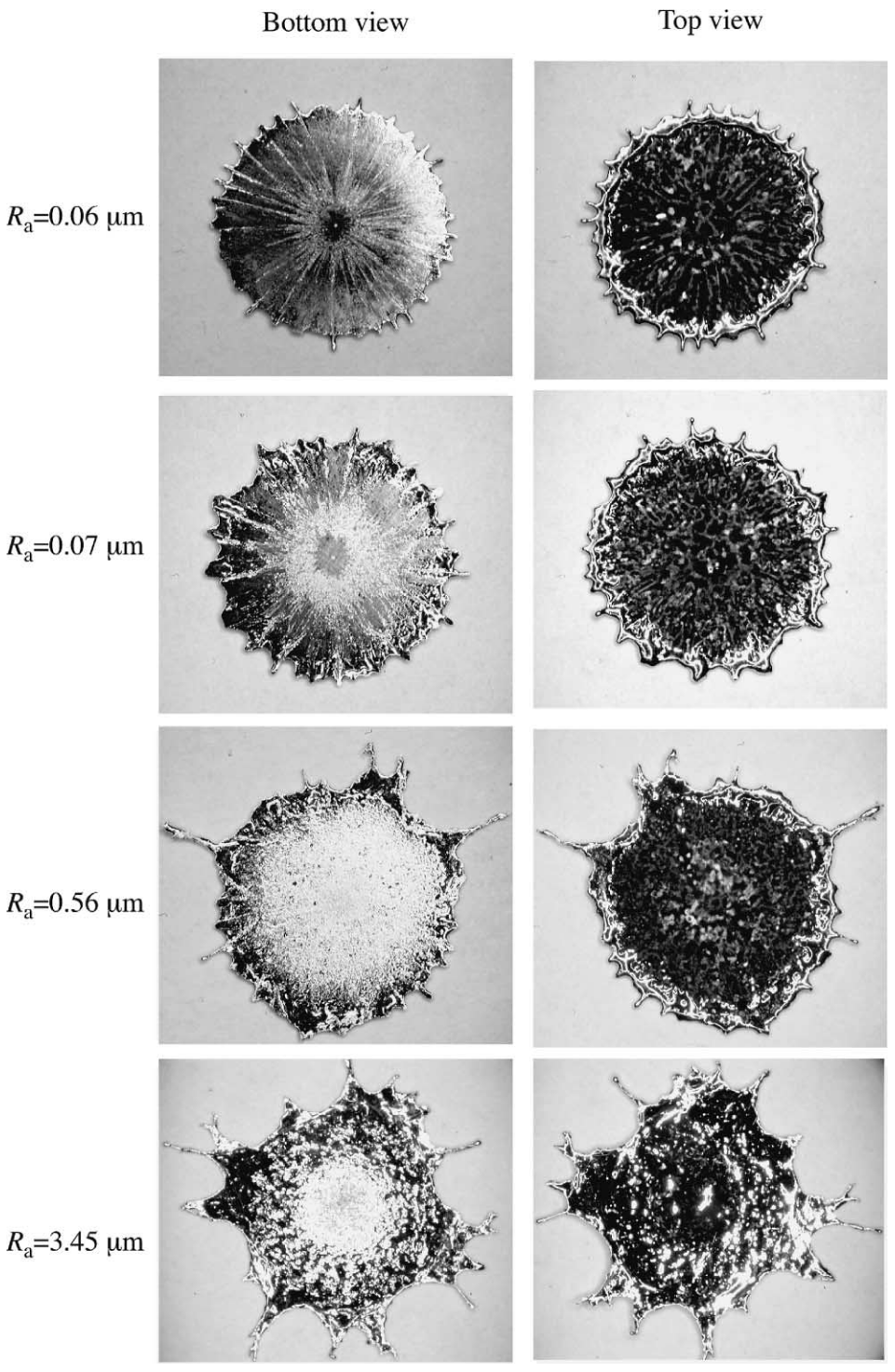

Fig. 9. Bottom and top view of splats after solidification on a stainless steel substrate at 25 °C with different surface roughness R_a.

found to be 140°: this value was used in all calculations. We did not observe any significant change of contact angle with surface roughness in our experiments. The work done in overcoming viscosity is [19]:

$$W = \frac{\pi}{3}\rho V_0^2 D_0 D_{\max}^2 \frac{1}{\sqrt{Re}} \tag{5}$$

If there is significant freezing during droplet impact, the kinetic energy of the frozen layer (of thickness s) is assumed to be lost:

$$\Delta\mathrm{KE} = \left(\frac{1}{2}\rho V_0^2\right)\left[\frac{\pi D_{\max}^2}{4}s\right] \tag{6}$$

The energy balance equation for this case is:

$$\mathrm{KE}_1 + \mathrm{SE}_1 - \Delta\mathrm{KE} = \mathrm{KE}_2 + \mathrm{SE}_2 + W \tag{7}$$

Substituting Eqs. (2)–(6) in Eq. (7), we obtain an expression for the maximum spread factor:

$$\xi_{\max} = \frac{D_{\max}}{D_0} = \sqrt{\frac{We + 12}{\frac{3}{8}We s^* + 3(1-\cos\theta) + 4\left(\frac{We}{\sqrt{Re}}\right)}} \tag{8}$$

where We is the Weber number ($We = \rho V_0^2 D_0/\sigma$) and Re is the Reynolds number ($Re = \rho V_0 D_0/\mu$). In our experiments these parameters were constant, with $Re = 31\,135$ and $We = 463$. s^* is the dimensionless solidified thickness ($s^* = s/D_0$) measured at the time the droplet is at its maximum spread. Pasandideh-Fard et al. [19] developed a simple model of droplet impact and estimated that the time taken for a liquid droplet to reach its maximum spread $t_{\max}$ is:

$$t_{\max} = \frac{8D_0}{3V_0} \tag{9}$$

For the values of $D_0 = 2.2$ mm and $V_0 = 4.0$ m/s used in the experiments, $t_{\max} = 1.46$ ms; Figs. 4 and 7 show that this is a reasonable order-of-magnitude estimate of the droplet spreading time, s^* can then be calculated from the analytical model of Garcia et al. [20], which calculates the thickness of the solidified layer in one-dimensional freezing of a melt in contact with a cold, solid surface, when there is thermal contact resistance at the interface.

To calculate the contact resistance we measured the maximum spread factor ($\xi_{\max}$) for droplets landing on each of the four surfaces of different roughness at 25 °C from Fig. 4. These values were substituted in Eq. (8) and s^* calculated. We then computed the value of contact resistance (R_c) corresponding to each value of s^* using the model of Garcia et al. [20]: the results of the calculation are shown in Fig. 10. Finally, Fig. 11 shows the variation of thermal contact resistance with surface roughness. R_c increased with surface roughness, with values lying in the range of $2–6 \times 10^{-6}$ m^2 K/W. These numbers are of the same magnitude as those measured previously by Pasandideh-Fard et al. [16] and Aziz and Chandra [12] who reported values lying in the range $1–5 \times 10^{-6}$ m^{2}K/W.

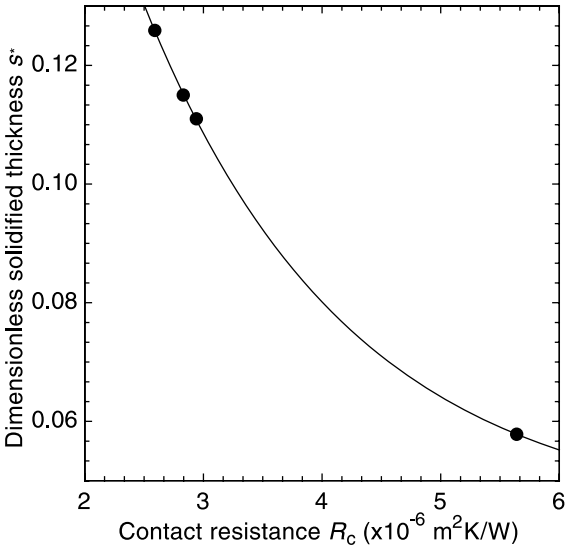

Fig. 10. Dimensionless solid layer thickness ($s^* = s/D_0$) variation with thermal contact resistance R_c.

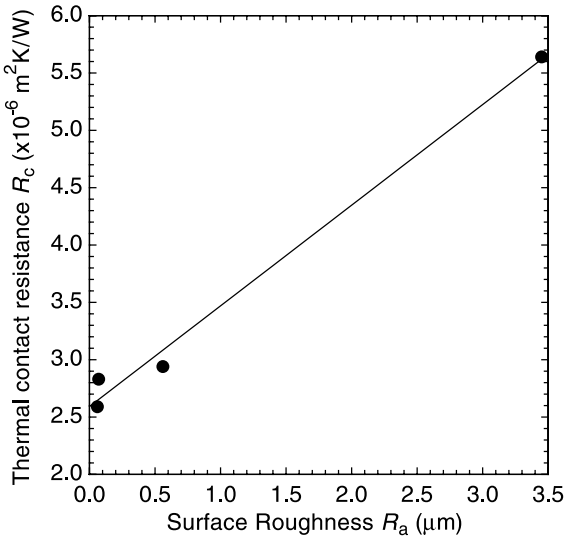

Fig. 11. Thermal contact resistance (R_c) variation with surface roughness (R_a) for 2.2 mm diameter tin droplets landing with an impact velocity of 4 m/s on a stainless steel surface at 25 °C.

3.5. Formation of fingers

Bhola and Chandra [11] and Aziz and Chandra [12] proposed a model for formation of fingers around an impacting droplet, which assumed that fingers were produced by a Rayleigh–Taylor instability, which occurs when the interface between two fluids of different density is accelerated. The number of fingers (N) that are formed around a splat at its maximum extent are:

$$N = \xi_{\max}\sqrt{\frac{We}{12}} \tag{10}$$

where $\xi_{\max}$ can be estimated from Eq. (8). On a hot surface, where there is no solidification, $s^* = 0$. Also, at velocities large enough to produce splashing, $We/\sqrt{Re} \gg 1$ and $We \gg 12$, so that Eq. (8) reduces to:

$$\xi_{\max} = \frac{Re^{1/4}}{2} \tag{11}$$

Substituting the above expressions for $\xi_{\max}$ into Eq. (10) gives:

$$N = \sqrt{\frac{We\sqrt{Re}}{48}} \tag{12}$$

Eq. (12) predicts $N = 41$ fingers for a 2.2 mm droplet impacting with a velocity of 4.0 m/s, which is close to the 44 fingers visible in Fig. 5 at $t = 2.3$ ms.

If the droplet is freezing as it lands then $\xi_{\max}$ has to be calculated from Eq. (8) after calculating the thickness of the frozen layer. Substituting this value in Eq. (10) gives $N = 24$, which compares well with the 29 fingers seen at $t = 2.0$ ms in Fig. 2.

Increasing surface roughness reduced the number of fingers (see Figs. 3 and 6), while making them larger. It became harder to count the fingers in this case, since they were not as clearly defined as they were on the smooth surface (e.g., Fig. 3b).

4. Conclusions

We photographed the impact of molten tin droplets on flat surfaces. Droplet spread factors and the numbers of fingers around splashing drops were measured from these photographs. The main conclusions that were drawn from this study are:

1. Tin droplets impacting on a surface at 240 °C splashed, with satellite droplets forming around their edges. Solidification arrested the formation of fingers when droplets impacted on a surface at 25 °C and reduced splashing.
2. Surface roughness had little effect on droplet spreading as long as the substrate temperature was above the melting point of tin. However on a cold surface, where droplets solidified during spreading, increasing surface roughness increased maximum spread diameter. This was attributed to the increase in thermal contact resistance with roughness, which reduces heat transfer from the droplet to the substrate and reduces the solidification rate.
3. Increasing substrate roughness from 0.06 to 0.56 μm increased the tendency to splash. Increasing roughness even more to 3.45 μm reduced the tendency to splash. This behaviour can be explained in terms of the competing effect of surface roughness and thermal contact resistance. On a smooth surface contact resistance is low, heat transfer is high, and the edges of the spreading droplet freeze quickly. The solidified edges perturb liquid flow and promote splashing. A rough surface has high contact resistance and therefore freezing is delayed until the droplet has spread out, reducing splashing.
4. The number of fingers formed around a droplet splashing on a smooth surface can be predicted reasonably well by a model based on the Rayleigh–Taylor instability.
5. Increasing surface roughness reduced the number of fingers while increasing their size.

References

[1] C.D. Stow, M.G. Hadfield, An experimental investigation of fluid flow resulting from the impact of a water drop with an unyielding dry surface, Proc. Royal Soc. A 373 (1981) 419–441.
[2] C. Mundo, M. Sommerfield, C. Tropea, Droplet–wall collisions: experimental studies of the deformation and breakup process, Int. J. Multiphase Flow 21 (1995) 151–173.
[3] A.L. Yarin, D.A. Weiss, Impact of drops on solid surfaces: self-similar capillary waves, and splashing as a new type of kinematic discontinuity, J. Fluid Mech. 283 (1995) 141–173.
[4] G.E. Cossali, A. Coghe, M. Marengo, The impact of a single drop on a wetted solid surface, Experim. Fluids 22 (1997) 463–472.
[5] B. Prunet-Foch, F. Legay, M. Vignes-Adler, C. Delmotte, Impacting emulsion drop on a steel plate:influence of the solid substrate, J. Colloid Interf. Sci. 199 (1998) 151–168.
[6] K. Range, F. Feuillebois, Influence of surface roughness on liquid droplet impact, J. Colloid Interf. Sci. 203 (1998) 16–30.
[7] R.F. Allen, The role of surface tension in splashing, J. Colloid Interf. Sci. 51 (1975) 350–351.
[8] S.T. Thoroddsen, J. Sakakibara, Evolution of the fingering pattern of an impacting drop, Phys. Fluids 10 (1998) 1359–1374.
[9] H.-Y. Kim, Z.C. Feng, J.-H. Chun, Instability of a liquid jet emerging from a droplet upon collision with a solid surface, Phys. Fluids 12 (2000) 531–541.
[10] M. Bussmann, S. Chandra, J. Mostaghimi, Modeling the splash of a droplet impacting a solid surface, Phys. Fluids 12 (2000) 3121–3132.
[11] R. Bhola, S. Chandra, Parameters controlling solidification of molten wax droplets falling on a solid surface, J. Mater. Sci. 34 (1999) 4883–4894.
[12] S.D. Aziz, S. Chandra, Impact, recoil and splashing of molten metal droplets, Int. J. Heat Mass Transfer 43 (2000) 2841–2857.
[13] M. Pasandideh-Fard, V. Pershin, I. Thomson, J. Mostaghimi, S. Chandra, Thermal spray coating formation: simu-

lations and experiments, Paper No. NHTC 2000-12181, National Heat Transfer Conference, Pittsburgh, Pennsylvania, 20–22 August, 2000.

[14] S. Schiaffino, A.A. Sonin, Molten metal deposition and solidification at low Weber numbers, Phys. Fluids 9 (1997) 3172–3187.

[15] D. Attinger, Z. Zhao, D. Poulikakos, An experimental study of molten microdroplet surface deposition and solidification: transient behavior and wetting angle dynamics, ASME J. Heat Transfer 122 (2000) 544–555.

[16] M. Pasandideh-Fard, R. Bhola, S. Chandra, J. Mostaghimi, Deposition of tin droplets on a steel plate: simulations and experiments, Int. J. Heat Mass Transfer 41 (1998) 45–49.

[17] M. Berg, J. Ulrich, Experimental-based detection of the splash limits for the normal and oblique impact of molten metal particles on different surfaces, J. Mat. Synth. Process. 5 (1997) 4549.

[18] S. Shakeri, Effect of substrate properties on molten metal droplet impact, Master of Applied Science Thesis, University of Toronto, 2001.

[19] M. Pasandideh-Fard, Y.M. Qiao, S. Chandra, J. Mostaghimi, Capillary effects during droplet impact on a solid surface, Phys. Fluids 8 (1996) 650–659.

[20] A. Garcia, T.W. Clyne, M. Prates, Mathematical model for unidirectional solidification of metals: II Massive moulds, Metall. Trans. B 10 (1979) 85–92.